



Enhanced mass sensitivity in novel magnetoelastic resonator geometries for advanced detection systems

Paula G. Saiz^{a,b}, David Gandia^{a,b}, Andoni Lasheras^b, Ariane Sagasti^b, Iban Quintana^c,
María Luisa Fdez-Gubieda^{a,b}, Jon Gutiérrez^{a,b}, María Isabel Arriortua^{a,b}, Ana Catarina Lopes^{a,*}

^a BCMaterials (Basque Center for Materials, Applications & Nanostructures), Bldg. Martina Casiano, 3rd. Floor, Barrio Sarriena s/n, 48940, Leioa, Spain

^b Universidad del País Vasco, UPV/EHU, Barrio Sarriena s/n, 48940, Leioa, Spain

^c Ik4-Tekniker, Polígono Tecnológico de Eibar, Calle Iñaki Goenaga, 5, Eibar, Spain

ARTICLE INFO

Keywords:

Magnetoelastic
Resonators
Sensitivity
Sensors
Geometries
Metglas

ABSTRACT

Acoustic wave based sensors have a major impact in the detection of low concentration of biological and chemical agents. Magnetoelastic resonator platforms are particularly interesting due to their low cost and wireless detection process. However, efforts in improving their performance are still focused only in the reduction of the size. In the present study, a new way to increase the sensitivity of magnetoelastic sensor platforms is proposed. This work demonstrates, both theoretically and experimentally, that the mass load sensitivity can be improved by tailoring sensor geometry and mass load position. Triangular and arched triangular shapes have been tested and compared with the traditional rectangular ones. It has been observed an increase in the mass sensitivity of more than 400% in Metglas[®] 2826MB magnetoelastic sensor by using new sensor platform geometries. Even higher sensitivities have been obtained by doing partial coatings on the sensor edge/tip instead of the traditional complete uniform coating. New geometries present an increase up to 6400% in partial coatings. The obtained results clearly show the key role of magnetoelastic resonator platforms geometries in the increase of mass load sensitivity and their importance in the draw of future labor-free and wireless sensors for low mass detection systems.

1. Introduction

The rapid and simple detection of very small quantities of different chemical or biological compounds in an accurate way is currently a demand in our society, mainly due to the health problems caused by their presence in air, water or food. Volatile Organic Compounds (VOCs) [1] or pathogenic microorganisms [2], for instance, could lead to several diseases making essential their control. Widely used methods for this detection are gas chromatography, flow cytometry, immunosensors, or culture tests, but they are labor-intensive, expensive and time consuming [3–5].

Alternatively, the use of acoustic wave based sensors turns out to be a good option due to their fast response compared to the traditional techniques. These devices are fabricated with a transducing material (the sensor platform) coated with a layer able to recognize the desired target. The detection process is based on the changes of the properties of an acoustic wave travelling through the sensor. The transducing material has a characteristic resonance frequency that is sensitive to different external parameters, such as mass perturbations, changing this

frequency when the active layer adsorbs the analyte to be detected. This change can be directly translated into an analyte mass change [6]. Some of the well known devices that are based on this operation principle are the Quartz Crystal Microbalance (QCM) and silicon microcantilevers. These kind of devices have already been reported to be useful for VOCs [7,8] or bacteria [9,10] detection. Despite the very high sensitivities of that systems, these are expensive and non-wireless detection instruments what limits the range of applications.

Following this detection principle, magnetoelastic resonators (MR) appear as an excellent alternative. They offer a quick remote detection of the target, with a cost efficiency and suitable for mass production. These magnetoelastic resonators have already been used as sensing platforms for different chemical and biological compounds or some other parameters such as viscosity, humidity, temperature or pressure [11–13]. Nevertheless, their sensitivity performance is still far from the ones presented by QCM and silicon microcantilever devices [7–10].

Magnetoelastic materials exhibit a strong dependence of their magnetic state under the application of any external force or mechanical load. Iron based amorphous ferromagnetic alloys are excellent

* Corresponding author.

E-mail address: catarinalopes83@gmail.com (A.C. Lopes).

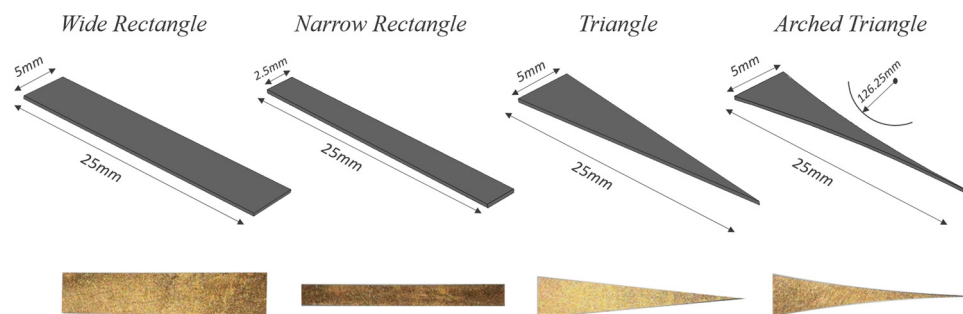


Fig. 1. (a) Scheme of the rectangular, triangular and arched triangular shape resonant platforms of 25 mm length and (b) images of the MR samples coated with gold.

magnetoelastic materials to be used for sensing purposes, both in the form of a magnetostrictive microcantilever or as a freestanding ribbon [14–16]. Nonetheless, when made of the same materials and with the same dimensions, the last one has a much higher sensitivity than the former [17]. When an external alternating excitation magnetic field is applied to a freestanding magnetoelastic ribbon a standing elastic wave travelling through it is induced. Matching the physical dimensions of the sensing material, the so called magnetoelastic resonance phenomenon (MER) appears. When a magnetoelastic ribbon is coated with a thin and uniform mass quantity (Δm), the shift in its resonance frequency (Δf) is given by [11]:

$$\frac{\Delta f}{f_0} = -\frac{1}{2} \frac{\Delta m}{m_0} \quad (1)$$

where f_0 is the magnetoelastic resonance frequency of the bare material and m_0 is the initial mass of the sensor. This relationship is just an approximation of a more general expression and it is not always valid to explain the frequency shift. For this reason, the obtained results are usually adjusted to other expanded equations [18,19]

The performance of this type of sensors is basically defined by its sensitivity, defined as $\Delta f/\Delta m$ [20]. Most of research in improving the sensitivity rely on reducing the size of the magnetoelastic resonant platform but keeping the usual rectangular geometry. This task is usually performed by using different methods such as polishing and dicing [21] or microelectronic fabrication techniques [22]. However, reducing the dimensions of the resonators to the microscale leads to additional problems such as edge defects, poor surface quality, loss of intensity in the signal or handling issues [23]. Thus, other solutions to improve the sensitivity avoiding the magnetoelastic platform size reduction are required. Recently, sensitivity measurements in triangular shape resonators have been reported [24], opening new perspectives in the goal of achieving high sensitive magnetoelastic platforms for biological detection.

Bearing all this in mind, a comprehensive and systematic study of the influence of different geometries in the mass sensitivity is proposed. Three different geometrical configurations will be tested: standard rectangular, triangular and arched triangular shaped ribbons. Moreover, we have also analysed the effect of partial mass loadings on the magnetoelastic ribbon sensitivity. For this purpose, strips of Metglas® 2826MB amorphous ferromagnetic alloy have been used. All the different shaped strips have been magnetically characterized, including resonance frequency and mass sensitivity measurements. Our results show a huge increase of the sensitivity from the rectangular to the triangular and arched triangular samples as well as a reduction of the sensory threshold to mass load located at outmost positions. Finally, the experimental results are supported by Finite Element Analysis (FEM) simulations. The knowledge achieved in this work is essential to improve the performance of future label-free and wireless sensors for low mass detection systems based on magnetolastic platforms.

2. Experimental

2.1. Materials and resonant platforms preparation

In this work, strips of the amorphous metallic glass Metglas® 2826MB alloy have been used. Meglas® 2826MB is a very common material used in magnetoelastic sensors applications due to its good magnetic and magnetoelastic properties such as its saturation magnetostriction (12 ppm) and saturation magnetization (0.88 T) [25]. EDX measurements were performed in order to obtain the composition of this alloy. The results show a wt% of 41, 48, 7 and 4% for Fe, Ni, Mo and B, respectively, what can be translated in the following atomic composition: $\text{Fe}_{37}\text{Ni}_{42}\text{Mo}_4\text{B}_{17}$. Besides, this alloy shows high corrosion resistance. All these properties as well as its low cost, make this alloy ideal to be used for different bio or chemical sensing applications [26].

Starting from a long ribbon of Metglas® 2826MB of 30 μm thick, free standing MR of 25 mm long were cut in rectangle, triangle and arched triangle (which curvature corresponds to a circumference with a radio of 126 mm) shapes, using a picosecond pulsed laser ablation technology (3D Macromac, microStruct). The use of this technique is crucial in order to obtain repeatability and avoid edge defects that are usually obtain when cutting with the micro dicing saw. Schemes of the different geometries used are shown in Fig. 1 as well as images of the used MR coated with gold.

2.2. Magnetoelastic characterization and mass load on MR surface

The resonance behaviour of the different sensor platforms was characterized using the magnetoelastic resonance detection system previously described [27]. Briefly, it consists on 2 coaxial solenoids, where the external solenoid generates the DC magnetic field for amplification of the signal through an HP 6653A DC power supply and the inner solenoid applies the AC magnetic field which drives the sample to the resonance. The induced signal in the magnetoelastic resonators is measured through a pick-up coil placed within the coaxial solenoids, which is then displayed in an HP3589A Spectrum Analyzer and recorded in the computer. All experiments were conducted at room temperature. In addition, the samples have been always placed in the same point in order to avoid possible deviations of the longitudinal axis among the different plat-forms.

The effect of mass deposition and subsequent analysis of the corresponding sensitivity was studied by sputtering a gold layer on the surfaces of the cleaned ribbons using a Quorum Q150TS turbo pumped coater. In order to determine the Au deposition rate (as mass/cm^2), a calibration curve was performed by using a high precision balance (0.1 μg sensitivity) after each deposition cycle. The mass loading deposition obtained with the used conditions (30 mA, 30 s) was $16 \pm 2 \mu\text{g}/\text{cm}^2$. It should be noted that the Metglas® 2826MB strips have one rough and one smooth side, due to their fabrication process. In order to keep systematic measurements, the Au mass deposition was always carried out in the smooth side of the ribbons.

After to clean all samples with acetone during 15 min in ultrasonic

bath, five consecutive gold layers were deposited. The depositions were performed covering different areas of the sensor surface. After each deposition, the gold coated samples were characterized by measuring the frequency shift in the magnetoelastic resonance curves.

2.3. Resonance frequency and mass sensitivity simulations

Theoretical simulations of the characteristic resonance frequency of the different sensor platform geometries, as well as simulations of the Au mass loads were carried out using Finite Element Analysis (FEM). The purpose of those simulations was to obtain the characteristic resonance frequency value of the pure longitudinal vibration for each sample in order to analyze the suitability of the proposed novel geometries. This task was performed through an eigenfrequency study. In this way, it must be noted that just pure elastic waves spreading along the different geometries are considered. First of all, the 3-D solid structures with the different geometries were defined. These built structures are free to move in any direction, without any constraint. Then, the elastic parameters of the Metglas® 2826MB (Young's modulus (E) of 152 GPa, density (ρ) of 7900 kg/m³ and Poisson's ratio (ν) of 0.33 [28]) were introduced and the simulated resonance frequency was obtained. Considering the magnetostrictive nature of this material and the consequent dependence of the Young's modulus on the external applied DC magnetic field (H), the value of 152 GPa was obtained thought the Eq. (3) and the results represented in Fig. 2-a for the wide rectangle, at the maximum of the magnetoelastic coupling (minimum of the graph). Since there is no other equation to calculate the Young's Modulus for these new geometries, the value obtained for the rectangle was extrapolated to the rest of geometries. Finally, in order to simulate the frequency shift under a mass load, a new layer was defined on the sensor surface with the elastic parameters of the gold given in the COMSOL materials library (Young's modulus (E) of 70 GPa, density (ρ) of 19,300 kg/m³ and Poisson's ratio (ν) of 0.44).

3. Results and discussion

3.1. Magnetoelastic characterization of the resonators

Magnetoelastic characterization of the different samples was performed in order to analyse the influence of novel shapes in those properties. The normalized variation of the resonance frequency as a function of the applied DC magnetic field is presented in Fig. 2(a). This is related with the well known ΔE effect, and its minimum occurs when the applied DC field is close to the anisotropy field (H_k) of the ferromagnetic ribbon. At this anisotropy field, the magnetoelastic coupling (energy interchange between elastic and magnetic energies) turns out to be maximum. Thus, all measurements concerning mass deposition sensitivity were performed at those applied external field values (see Table 1).

ΔE values can be calculated from Fig. 2(a) considering Eq. (2):

$$\Delta E = \frac{E_s - E_{min}}{E_s} \times 100 \quad (2)$$

where E_s is the Young modulus at the magnetic saturation state and E_{min} is the minimum value of the Young modulus. Both are directly related with the resonance frequencies at that points by the Eq. (3):

$$E(H) = \rho (n2Lf_r)^2 \quad (3)$$

being ρ the density of the MR, n the resonance mode number ($n = 1$) and L the length of the MR.

The calculated values of ΔE effect for the different samples are represented in Table 1. Despite not very significant, some differences can be appreciated in the values of ΔE effect as well as on the bias field (H) required to maximize it. The wider rectangular ribbon presents the lower value of ΔE (2.7%), followed by the triangular and arched triangular shaped samples (3.2%) and finally by the narrow rectangle

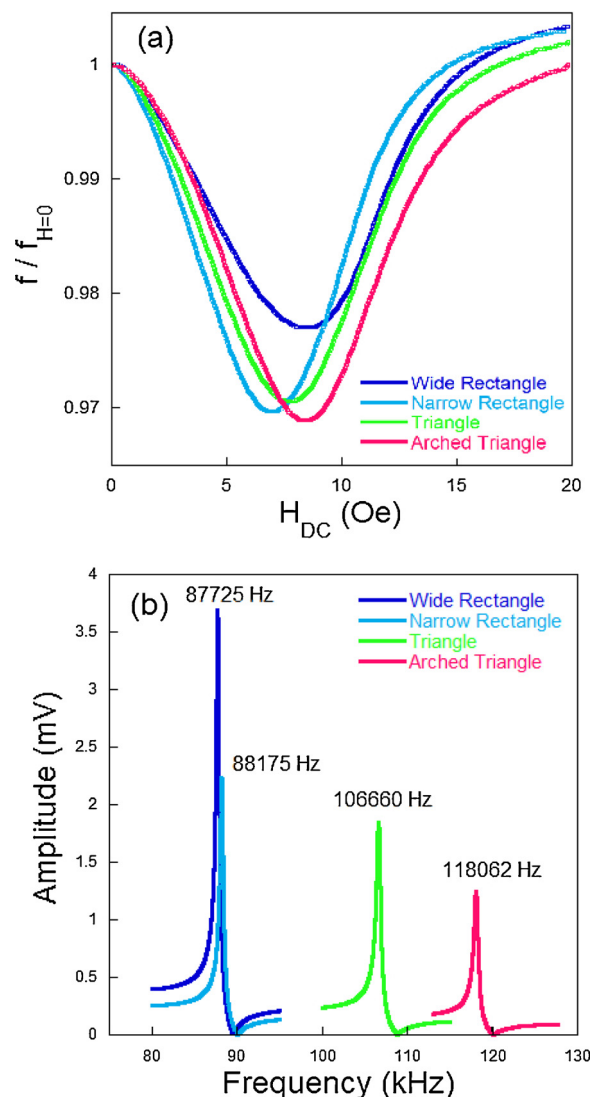


Fig. 2. (a) Variation of the magnetoelastic resonance frequencies as a function of applied magnetic bias field for the different sensor platforms (b) Magnetoelastic resonance curves of all the samples, measured at the corresponding field.

Table 1

Resonance frequency (f_0), ΔE effect (ΔE), Quality factor (Q), Magnetoelastic coupling coefficient (k) and applied bias field (H) of the bare resonant platforms.

Sample	f_0 (Hz)	ΔE (%)	Q	k	H (Oe)
Wide Rectangle	87725	2.7	158.1	0.225	8.5
Narrow Rectangle	88175	3.4	141.1	0.225	7.1
Triangle	106660	3.2	139.2	0.224	7.7
Arched Triangle	118062	3.2	149.6	0.207	8.5

(3.4%). Moreover, a lower value of H is presented by the narrow rectangle (7.1 Oe), followed by the triangular shaped sample (7.8 Oe). Finally, both wide rectangle and arched triangle samples present the highest value of H (8.5 Oe). These differences are probably related to the demagnetizing field. In the case of rectangular shaped resonators this is homogeneous along the platform and is higher for lower length to width ratio of the sample [29]. Thus, the increase of ΔE effect as well as the reduction of H from the wide to the narrow rectangle could be expected. Moreover, in the case of new geometries, the demagnetization field is probably not uniform all over the platform, which results in

a non uniform effective magnetic field in these platforms. This fact is also probably in the origin of the different values of H needed to maximize the ΔE effect of these samples. Furthermore, the increase of the ΔE effect in the non-rectangular shaped samples indicates that the resonant platform geometry can also play an important role on the demagnetizing field.

The resonance curves of all the samples are shown in Fig. 2(b). From those curves, three important magnetoelastic parameters that define the good performance of the sensor can be obtained: the initial resonance frequency (f_0), the quality factor (Q), and the magnetoelastic coupling coefficient (k). Where the quality factor is calculated from equation (4) [27]:

$$Q = \frac{f_0}{\Delta f} \quad (4)$$

with f_0 the resonance frequency and Δf the full width at half maximum intensity. Finally, the magnetoelastic coupling is obtained from:

$$k^2 = \frac{\pi^2}{8} \left[1 - \left(\frac{f_0}{f_a} \right)^2 \right] \quad (5)$$

where f_0 is the resonance frequency and f_a the antiresonance frequency. All the obtained parameters are shown in Table 1.

As expected, the resonance frequency of the wide and narrow rectangles present very similar values (87725 and 88175 Hz respectively), despite the lower resonance amplitude of the narrow rectangle. In the case of the triangle and arched triangle geometries, a significant increase of their resonance frequency (f_0) is observed if compared with the rectangular shaped ones. As in the case of the narrow rectangle, there is a decrease in the signal of the resonance amplitude, which is attributed to the less amount of magnetoelastic material. However, the sharpness of the peak is not significantly affected, as it can be confirmed by the similar values of obtained quality factor. Regarding the magnetoelastic coupling coefficient, no significant changes were observed among the different samples. Thus, it can be concluded that the main magnetoelastic parameters of the ribbons are not affected by the change in the geometry, which leads to explore the performance of these novel resonators under the action of different external agents.

3.2. Mass sensitivity of the different shaped magnetoelastic resonators

After the initial characterization of all the proposed resonators, the influence of the different geometries on their mass deposition sensitivity was studied. For that purpose, 5 successive depositions of gold were performed by vacuum sputtering on the whole sensor surface of the MR, using the procedure previously described in section 2.2. After each deposition, the magnetoelastic resonance frequency value was measured. The obtained variation in the magnetoelastic resonance frequency as a function of the successive mass loading for each sample is shown in Fig. 3.

The obtained slope for each geometry case gives the experimental mass sensitivity, S . Results are summarized in Table 2 together with the initial frequencies and masses of all the MR and with the mass loaded in each deposition.

The wide rectangular MR presents a sensitivity of 1.22 Hz/ μ g. This value is almost doubled in the case of the narrow rectangular strip (2.22 Hz/ μ g) and further increases of more than 270% and 435% are observed when using the triangular and arched triangular shaped strips, respectively. Considering Eq. (1), the increase of the mass sensitivity from the wide to the narrow rectangular resonant platform could be expected due to the reduction of its mass. However, despite the mass of the rectangular narrow MR and the triangular MR is the same, the triangular one is much more sensitive to the mass deposition. This clearly demonstrates that the sensitivity can be also tailored by changing the MR geometry, which is associated to the increase of the magnetoelastic resonance frequency of the different geometries.

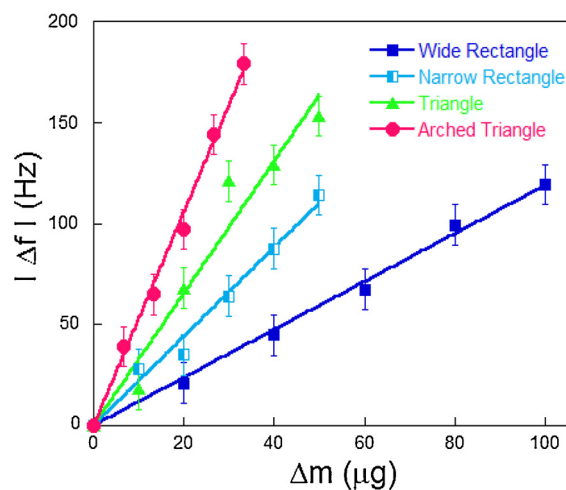


Fig. 3. Shift on the resonance frequency under a specific change in mass for the different sensor platforms geometries completely coated.

Table 2

Initial mass (m_0), experimental resonance frequency (f_0), simulated resonance frequency ($f_{0\text{ sim}}$), mass loaded on each deposition (Δm) and mass sensitivity (S) for the different resonant platforms.

Sample	m_0 (mg)	f_0 (Hz)	$f_{0\text{ sim}}$ (Hz)	Δm (μ g)	S (Hz/ μ g)
Wide Rectangle	31.6468	87725	87565	20.000	1.22
Narrow Rectangle	15.5261	88175	87688	10.000	2.22
Triangle	15.9108	106660	106540	10.000	3.29
Arched Triangle	11.3751	118062	124850	6.645	5.34

Therefore, the lower mass of the arched triangle shaped MR together with its higher resonance frequency value, results in the highest measured sensitivity S .

3.3. Theoretical resonance behavior of the MR

The traditional rectangular shaped MR is a symmetric and very well known system. Several studies describe its mass sensitivity behaviour as well as its dependence with mass load distribution. Instead, everything remains to be studied for non-rectangular MR sensors. In this way, in order to deep our knowledge about these samples and look for possibilities to improve even more the sensitivity, computer simulations were done using the commercially available COMSOL Multiphysics® software program. The first resonance frequency mode as well as the shift on the frequency for a given mass load were simulated for all the samples. The simulated vibrations for the different geometry samples are shown in Fig. 4.

In Fig. 4, the different colors represent the displacement that the magnetoelastic resonators undergo at the obtained resonance frequency. Results for the resonance frequencies simulated together with the experimental results are shown on Table 2.

It can be appreciated that the results obtained from the simulations are very similar to the experimentally measured ones. The slight differences observed can be attributed to some deviations between the pure elastic wave, considered in the simulation, and the magnetoelastic wave measured experimentally. This magnetoelastic wave is a direct consequence of the magnetoelastic coupling, which plays a key role in this aspect [30]. However, as cited before, the Young's Modulus value used in the simulation was the same for all the used geometries, despite the value has been calculated only for the rectangular one. This fact can be in the origin of the higher (although small) variations observed between the experimental and simulated frequency values of the triangular and arched triangular shaped samples.

Looking at the results, additional information stands out. Despite

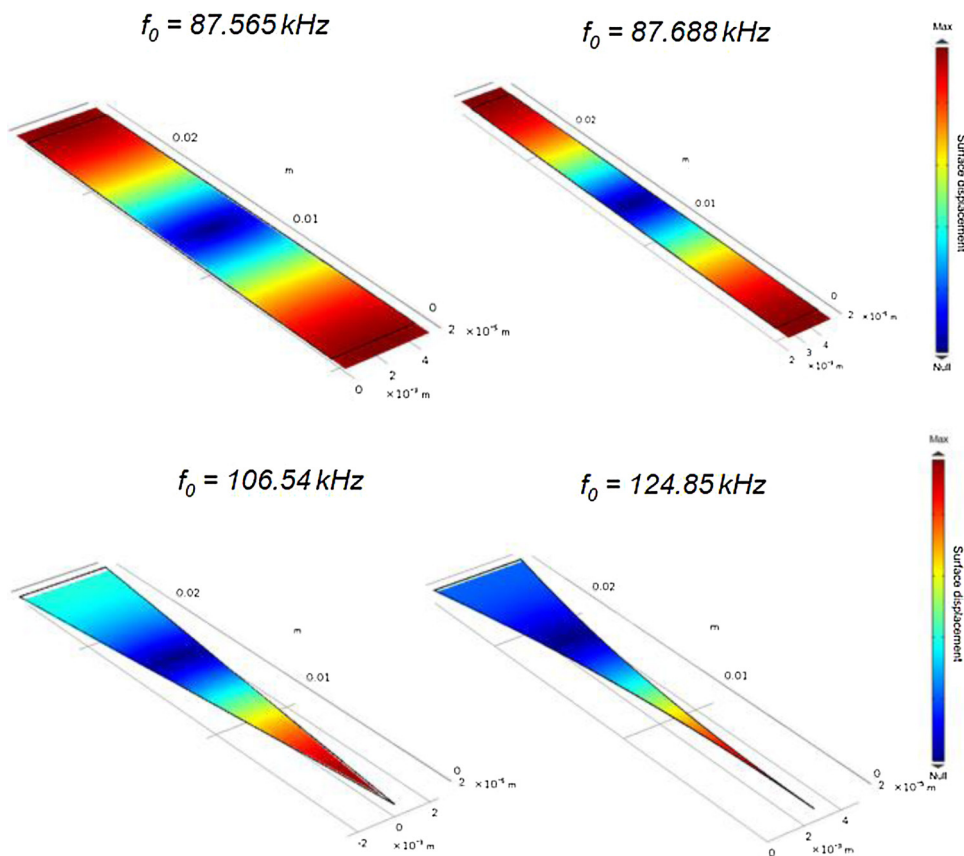


Fig. 4. Images of the resonance frequency simulations for the different samples.

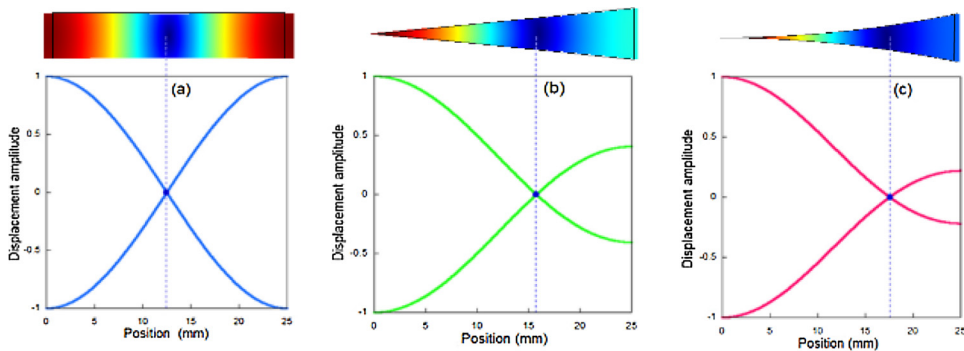


Fig. 5. Normalized total displacement at the different zones of the sensor platform for: (a) Both rectangular shape MRs, (b) the triangular shape MR, and (c) the arched triangular shape MR.

most of the studies distribute the mass load uniformly all over the MR surface, according to the results showed in Fig. 4, the deformation is not uniform. Actually, the rectangular sample vibrates around a nodal point placed in the center of the strip. At this point (in dark blue), the displacement is null and on the contrary, it is maximum at the edges of the ribbon (in red). In the case of triangular and arched triangular shaped MR, however, an asymmetric distribution of the deformation is observed as a direct consequence of their asymmetric shape. The node position is displaced to a further position from the tip, being at this end the highest deformation. The normalized total displacement as function of the distance from the edge/tip of the different sensors is shown in Fig. 5.

As it can be observed, the position of the nodal point depends on the sample geometry. For both rectangles, the node is located at the center (12.5 mm), while for the triangle and arched triangle shaped samples this position is displaced from the center point to approximately 16 mm

and 17.5 mm, respectively. Considering these different obtained elongations and some previous studies [31,32], it can be predicted that the different zones of the sensor surface will not be equally sensitive. Moreover, if the nodal point is further from the tip in the triangle and in the arched triangle shaped resonators, the tip of these sensors should be much more sensitive than the edges of the rectangular ones. Keeping all this in mind, not only deposition of a uniform coating on the whole surface of the MR, but also partial coatings were performed and compared with theoretical simulations. Obtained experimental and theoretical results are shown in the following section.

3.4. Sensitivity dependence with coated surface

An exhaustive experimental study of the dependence of mass sensitivity with the coated area was carried out following the same coating procedure described in section 2.2. The depositions were performed

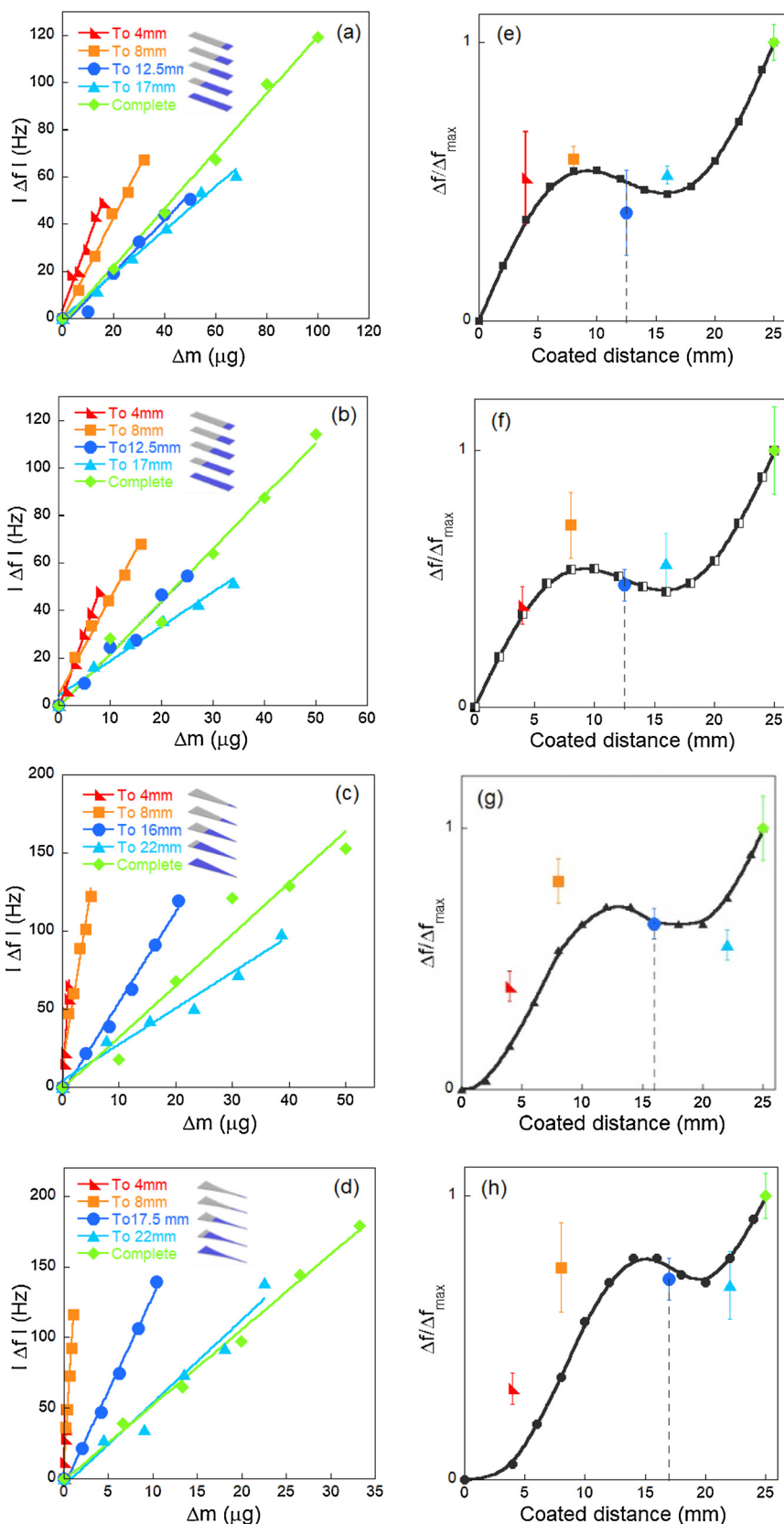


Fig. 6. Frequency shift at different distances from the edge/tip as a function of the mass load deposition obtained experimentally (a–d). Normalized frequency shift as a function of the different distances obtained by computer simulations (e–h, black line). Normalized experimental results of the average frequency shift obtained for the different depositions are also represented in color points on Figs. 6(e–h). Wide rectangle (a and e), narrow rectangle (b and f), triangle (c and g) and arched triangle (d and h) shaped MRs.

from the edge (wide and narrow rectangular shaped MR) or the tip (triangular and arched triangular shaped MR) to 4 mm, 8 mm, the node position and 25 mm of the resonant platform (see insets in Figs. 6 (a–d)). Moreover, a mass deposition beyond the node (to 17 mm for both rectangles and to 22 mm for the triangular and arched triangular shape samples) was carried out. The experimentally measured variation of the resonance frequency value for each coated distance as function of the mass change is shown in the Fig. 6 (a–d). Additionally, partial depositions of 90 nm layers on the surface of the MRs were also simulated, for comparison. Considering the differences between the experimental and simulated thickness of deposited layer (5×15 nm and 90 nm, respectively), the variation of resonance frequency values were normalized by dividing the value of a resonance frequency at a specific coat distance of MR (Δf) by the value at a complete coat MR (Δf_{\max}). This variation is represented as a function of the coated distance (measured from the edge) which is shown in Fig. 6 (e–h). The black points and line correspond to simulated results while the color points correspond to the normalized frequency shift obtained experimentally from the Figs. 6 (a–d).

As can be observed, the performed simulations show that until a specific value of the coated distance, the resonance frequency shift increases as the coated distance does. Considering Eq. (1) and taking into account that we are increasing the loaded mass, these results were expected. Nevertheless, when the mass deposition distance is reaching the position of the vibration node of the sample, the frequency shift stabilizes. Moreover, the frequency shift even decreases at a point below the nodal point of each sensor (9.3, 13.2 and 15.5 mm for the rectangular, triangular and arched triangular shape samples, respectively). Finally, for a subsequent increase of the coated distance, the variation of the frequency value increases again, reaching its maximum when the totality of the MR is coated. This behavior clearly manifests that the mass sensitivity depends on the coated area of the sensor. In the same way, the obtained results show that a higher amount of mass loaded not always results in a higher variation of resonance frequency value. At the same time, the equivalent experimental measurements performed, show a similar trend as the simulated results, Fig. 6 (a–d).

Furthermore, from the different slopes of the results in Fig. 6 (a–d), it could be observed that the sensitivity, $S = \Delta f / \Delta m$, is dependent on the coated surface of the sample. The experimental results of sensitivity as a function of the amount of coated surface are represented in Fig. 7(a). However, being aware of the few numbers of experimental points presented, a COMSOL simulation was performed in order to reproduce the partial gold depositions at a larger number of different coated distances. These results are presented in Fig. 7(b). It is observed that the sensitivity decreases as the amount of coated surface increases. Moreover, it can be appreciated in the case of rectangular and triangular shaped samples, a minimum in the sensitivity when the deposition transcends the distance of the nodal point (inset Fig. 7(a) and 7(b)) however it increases again when the entire surface of the strip is covered. This behavior has already been observed for the well studied rectangular geometry [33]. Nonetheless, the decrease on the minimum mass quantity that the MR can detect (mass sensory threshold) close to the tip becomes much more remarkable in these new geometries (triangular and arched triangular shaped). From the obtained experimental values, it can be seen that the sensitivity of the MR when 4 mm of edge/tip are coated is increased by about 250, 1620 and 6400% for the rectangular, triangular and arched triangular shaped samples, respectively, if compared with the completely covered MR.

Again, the trend of the mass sensitivity values is quite similar for both theoretical and experimental results at large coated distances. Nonetheless, some significant discrepancies in the absolute values are observed at small coated distances. In this case, the sensitivities obtained experimentally are bigger than the ones obtained by simulations. These differences can be attributed to the higher experimental measurement error for small coated distances when compared with the complete coated samples. Additionally, previous studies show the

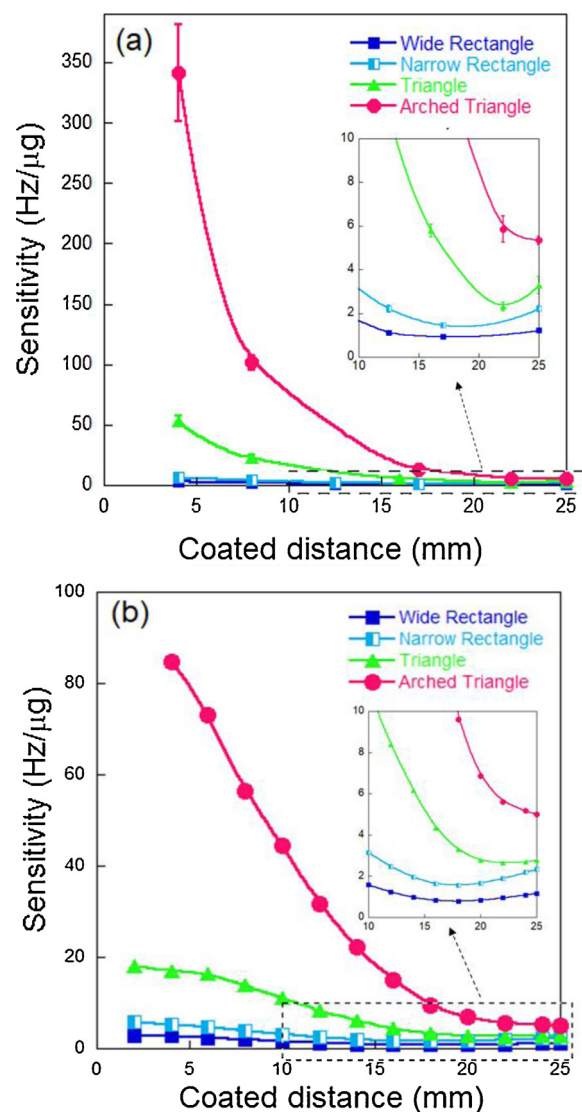


Fig. 7. Sensitivity as a function of the coated distance for the different samples obtained: (a) experimentally and (b) by computer simulations. Inset: Detail of the lowest mass sensitivity response indicated by the rectangular box.

dependence of mass sensitivity with the properties of the material that is used in the coating process, particularly the dependence on their elastic properties [34]. Thus, the differences of elastic properties between the sputtered gold layer used in the experimental measurements and the perfectly uniform and compact gold sheet simulated are also in the basis of this discrepancies [30].

Considering the results presented in this work, it is clear the key role that the shape of the MR plays in the increase of mass load sensitivity. Furthermore, this work is fundamental to understand that the total coverage of the platform is the optimal way to obtain a higher variation in the frequency shift, while a tip located load mass represents a huge reduction of mass sensory threshold. The last paves the way for the detection, for example, of a single pathogen agent.

4. Conclusions

In this work it was studied the role of magnetoelastic resonant platforms geometry on its load mass sensitivity. Theoretical and experimental measurements have been performed in order to compare the performance of the two new geometries (triangular and arched triangular ones) with respect to the traditional rectangular one. The use of

triangular and arched triangular shaped MR results in an increase of their magnetoelastic resonance frequency that in turn is translated in the increase of their mass load sensitivity. Compared to the rectangular MR, that increase is of more than 270% and 435% in the triangular and arched triangular shaped samples, respectively.

Moreover, it was also noticed that the sensitivity is improved by partial coatings at the edge/tip of the magnetoelastic resonant platform when compared to the traditional full covered surface. Again, this fact is more remarkable on the triangular and arched triangular shape sensors with respect to the rectangular one. Comparing the tip/edge coated (until a distance of 4 mm) with the complete coated sample (until a distance of 25 mm), an increase of about 250, 1620 and 6400% in the sensitivity has been observed for the rectangular, triangular and arched triangular shaped sensors, respectively. These results are particularly interesting since lead to a huge reduction of mass sensory threshold, which for sure will facilitate the possible detection of a single agent.

The possibility of increasing the sensitivity by playing with the geometry and with partial MR coatings, combined with the reduction on the MR platform size will give rise to excellent high sensitive, cheap and wireless sensors, which will extend the range of their applications.

Acknowledgements

This work was financially supported by the “Ministerio de Economía, Industria y Competitividad” (MAT2016-76739R(AEI/FEDER, UE)) and by the “Gobierno Vasco”, under projects IT-630-13 (Basque University Research System Groups), ACTIMAT KK-2018/00099 and muF4 KK-2017/00089 (Elkartek Program). A.C.Lopes thanks to MSCA-IF-2015 (Marie Skłodowska Curie Actions) of the European Union's Horizon 2020 Programme for the received funds under grant agreement n° [701852].

References

- H. Guo, S.C. Lee, L.Y. Chan, W.M. Li, Risk assessment of exposure to volatile organic compounds in different indoor environments, *Environ. Res.* 94 (1) (2004) 57–66.
- T. Martinović, U. Andjelković, M.Š. Gajdošik, D. Rešetar, D. Josic, Foodborne pathogens and their toxins, *J. Proteomics* 147 (2016) 226–235.
- A.C. Soria, M.J. García-Sarrió, A.I. Ruiz-Matute, M.L. Sanz, Headspace techniques for volatile sampling, *Compr. Anal. Chem.* 76 (2017) 255–278.
- Z. Shen, M. Huang, C. Xiao, Y. Zhang, X. Zeng, P.G. Wang, Nonlabeled quartz crystal microbalance biosensor for bacterial detection using carbohydrate and lectin recognitions, *Anal. Chem.* 79 (6) (2007) 2312–2319.
- D. Rodríguez-Lazaro, B. Lombard, H. Smith, A. Rzezutka, M. D'Agostino, R. Helmuth, A. Schroeter, B. Malorny, A. Miko, B. Guerra, J. Davison, A. Kobilinsky, M. Hernandez, Y. Bertheau, N. Cook, Trends in analytical methodology in food safety and quality: monitoring microorganisms and genetically modified organisms, *Trends Food Sci. Technol.* 18 (2007) 306–319.
- R.B. Priya, T. Venkatesan, G. Pandiyarajan, H.M. Pandya, A short review of SAW sensors, *J. Environ. Nanotechnol.* 4 (4) (2015) 15–22.
- Y. Dong, W. Gao, Q. Zhou, Y. Zheng, Z. You, Characterization of the gas sensors based on polymer-coated resonant microcantilevers for the detection of volatile organic compounds, *Anal. Chim. Acta* 671 (2010) 85–91.
- A.H. Khoshaman, B. Bahreyni, Application of metal organic framework crystals for sensing of volatile organic gases, *Sensors Actuators B. Chem.* 162 (2012) 114–119.
- J. Wang, M.J. Morton, C.T. Elliott, N. Karoonuthaisiri, L. Segatori, S.L. Biswal, Rapid detection of pathogenic bacteria and screening of phage-derived peptides using microcantilevers, *Anal. Chem.* 86 (2014) 1671–1678.
- C. Yao, T. Zhu, J. Tang, R. Wu, Q. Chen, M. Chen, B. Zhang, J. Huang, W. Fu, Hybridization assay of hepatitis B virus by QCM peptide nucleic acid biosensor, *Biosens. Bioelectron.* 23 (2008) 879–885.
- C.A. Grimes, S.C. Roy, S. Rani, Q. Cai, Theory, instrumentation and applications of magnetoelastic resonance sensors: A review, *Sensors* 11 (2011) 2809–2844.
- T. Baimpos, L. Gora, V. Nikolakis, D. Kouzoudis, Selective detection of hazardous VOCs using zeolite/Metglas composite sensors, *Sensors Actuators, A Phys.* 186 (2012) 21–31.
- S. Huang, H. Yang, R.S. Lakshmanan, M.L. Johnson, J. Wan, I.-H. Chen, H.C. Wikle III, V.A. Petrenko, J.M. Barbaree, B.A. Chin, Sequential detection of Salmonella typhimurium and Bacillus anthracis spores using magnetoelastic biosensors, *Biosens. Bioelectron.* 24 (2009) 1730–1736.
- J. Gutierrez, J.M. Barandiaran, O.V. Nielsen, Magnetoelastic Properties of Some Fe-Rich Fe-Co-Si-B metallic glasses, *Phys Stat Sol* 111 (1989) 279.
- J.M. Barandiaran, J. Gutierrez, E. Garcia-Arribas, Magneto-elasticity in amorphous applications and materials science ferromagnets: Basic principles and applications, *Phys. Status Solidi* 2264 (10) (2011) 2258–2264.
- Suiqiong Li, Fu Liling, J.M. Barbaree, Z.-Y. Cheng, “Resonance behavior of magnetostrictive micro/milli-cantilever and its application as a biosensor”, *Sensors and Actuators B: Chemical* 137 (2) (2009) 692–2699.
- Kewei Zhang, Lin Zhang, Liling Fu, Suiqiong Li, Huiqin Chen, Z.-Y. Cheng, Magnetostrictive resonators as sensors and actuators, *Sens. Actuators A Phys.* 200 (2013) 2–10.
- A. Sagasti, J. Gutiérrez, M.S. Sebastián, J.M. Barandiarán, Magnetoelastic Resonators for Highly Specific Chemical and Biological Detection: A Critical Study, *IEEE Trans. Magn.* 53 (4) (2017) 10–13.
- R. Madhumidha, B.C. Porok, Resonance behavior of magnetostrictive sensor in biological agent detection, *Experimental and Applied Mechanics* (2010) 1–7. IMECE2010-37162.
- W. Shen, R.S. Lakshmanan, L.C. Mathison, V.A. Petrenko, B.A. Chin, Phage coated magnetoelastic micro-biosensors for real-time detection of Bacillus anthracis spores, *Sensors Actuators, B Chem.* 137 (2009) 501–506.
- R.S. Lakshmanan, R. Guntupalli, J. Hu, V.A. Petrenko, J.M. Barbaree, B.A. Chin, Detection of Salmonella typhimurium in fat free milk using a phage immobilized magnetoelastic sensor, *Sensors Actuators, B Chem.* 126 (2) (2007) 544–550.
- M.L. Johnson, J. Wan, S. Huang, Z. Cheng, V.A. Petrenko, D.-J. Kim, I.-H. Chen, J.M. Barbaree, J.W. Hong, B.A. Chin, A wireless biosensor using microfabricated phage-interfaced magnetoelastic particles, *Sensors Actuators, A Phys.* 144 (2008) 38–47.
- M.L. Johnson, O. LeVar, S.H. Yoon, J.-H. Park, S. Huang, D.-J. Kim, Z. Cheng, B.A. Chin, Dual-cathode method for sputtering magnetoelastic iron-boron films, *Vacuum* 83 (2009) 958–964.
- N. Pacella, A. Derouin, B. Pereles, K.G. Ong, Geometrical modification of magnetoelastic sensors to enhance sensitivity, *Smart Mater. Struct.* 24 (2015) 025018.
- Metglas® (Noviembre 2018). www.metglas.com, <https://metglas.com/wp-content/uploads/2016/12/2826MB-Technical-Bulletin.pdf>.
- R.S. Lakshmanan, R. Guntupalli, J. Hu, D.-J. Kim, V.A. Petrenko, J.M. Barbaree, B.A. Chin, Phage immobilized magnetoelastic sensor for the detection of Salmonella typhimurium, *J. Microbiol. Methods* 71 (2007) 55–60.
- A.C. Lopes, A. Sagasti, A. Lasheras, V. Muto, J. Gutiérrez, D. Kouzoudis, J.M. Barandiaran, Accurate Determination of the Q quality factor in magnetoelastic resonant platforms for advanced biological detection, *Sensors* 18 (2018) 887.
- C.P. Chou, L.A. Davis, R. Hasegawa, Elastic constants of Fe (Ni, Co)-B glasses, *J. Appl. Phys.* 50 (5) (1979) 3334–3337.
- C.A. Grimes, C.S. Mungle, K. Zeng, M.K. Jain, W.R. Dreschel, M. Paulose, K.G. Ong, Wireless magnetoelastic resonance sensors: A critical review, *Sensors* 2 (2002) 294–313.
- S. Schmidt, C.A. Grimes, Characterization of nano-dimensional thin-film elastic moduli using magnetoelastic sensors, *Sensors Actuators, A Phys.* 94 (2001) 189–196.
- S. Li, Z. Cheng, Nonuniform mass detection using magnetostrictive biosensors operating under multiple harmonic resonance modes, *J. Applied Physics* 114514 (2010) 2013.
- K. Zhang, L. Zhang, Y. Chai, Mass load distribution dependence of mass sensitivity of magnetoelastic sensors under different resonance modes, *Sensors* 15 (2015) 20267–20278.
- K. Zhang, K. Zhang, Y. Chai, Study of ‘blind point’ and mass sensitivity of a magnetostrictive biosensor with asymmetric mass loading, *AIP Adv.* 4 (2016) 0571142014.
- R. Zhang, M.I. Tejedor-Tejedor, C.A. Grimes, M.A. Anderson, Measuring the mass of thin films and adsorbates using magnetoelastic techniques, *Anal. Chem.* 79 (18) (2007) 7078–7086.

Paula G. Saiz, Graduate in Physics and Master in New Materials in 2017, is currently pursuing her PhD at the BCMaterials Research Center. During her career she had acquire skills in different areas of materials. In particular, she has extensive experience in various methods of synthesis and in different characterization techniques (X-Ray diffraction, scanning electron microscopy, thermogravimetric analysis, mechanical testing, IR spectroscopy, magnetic and magnetoelastic characterization...). She has presented his works in several conferences and is member of the IEEE Magnetic Society and the American Physical Society (APS). Her current research activities are focus on the development of functionalized magnetoelastic resonators for Volatile Organic Compounds detection using porous materials as sensing layers and in the improvement of the properties of that sensing devices.

David Gandia obtained his Degree in Physics from the Universidad del País Vasco (UPV/EHU) in 2016, and afterwards he enrolled in the Interuniversity Master of New Materials, offered by the Universidad de Cantabria (UC) and the Universidad del País Vasco (UPV/EHU). In his Bachelor's Final Year and master's Degree Projects he has been working with the Group of Magnetism and Magnetic Materials, collaborating with the Immunology, Microbiology and Parasitology department, in an interdisciplinary research project related to Magnetotactic Bacteria for Enhanced Applications. In this project he has developed a method to create 2D and 3D arrays of magnetotactic bacteria for data storage applications and theoretical studies, and in addition, he has also analyzed the viability of these bacteria as nanorobots for Magnetic Hyperthermia mediated Cancer Treatment.

Andoni Lasheras is Assistant Professor in the Applied Physics I Department at the Faculty of Engineering of the University of the Basque Country. He got his degree on Physics at the University of the Basque Country (Spain) in 2009 and completed the Master on New Materials in 2010. In 2012, he obtained a PhD fellowship from de Basque Government to develop a work based on the magnetoelectric effect in magnetostrictive/piezoelectric

laminates composites, which successfully finished in January 2016. His research interests are focused on magnetoelastic and magnetoelectric materials for sensing applications and energy harvesting devices. He has published about 27 scientific papers in peer-reviewed journals, as well as to participate in several international conferences with both poster and oral contributions. He collaborates with several national and international research groups and he is currently member of the scientific committee of the International Conference on Material Engineering and Smart Materials. He also served as Guest Editor in the Materials journal for the Special Issues related to magnetic and magnetoelastic sensors.

Ariane Sagasti is graduated in Chemistry in 2011 and Master in New Materials in 2012, both at the University of the Basque Country. She received her PhD in Material Science and Technology in March 2018 at the BCMaterials Research Center. During the development of the thesis work about functionalization of magnetoelastic resonant platforms for chemical and biological sensing purposes she spent 4 months at the University of Patra, in Greece. She has expertise working with different materials (metallic alloys, polymers, zeolites, oxides...), synthesizing them through different routes and characterizing (XRD, SEM, EDX, DSC, voltammetry, electrochemical measurements, magnetic and magnetoelastic characterization...). Nowadays she is focused on improving the corrosion resistance of the magnetoelastic sensors for biological detection.

Iban Quintana obtained his PhD in Materials Physics at the Universidad del País Vasco (UPV – EHU) and the Donostia International Physics Centre (DIPC) in 2007. His work was focused on the study of the effect of temperature on the molecular dynamic and on the properties of transport in thermoplastics used as membranes. In 2007 he joined IK4-Tekniker, working in the study of microfabrication processes by pulsed laser of short and ultrashort duration. In 2007 he realized a post-doctoral secondment in Manufacturing Engineering Center (Cardiff) where he studied a theoretical and experimental study about the effect of laser radiation in metallic glasses. He is author of more than 20 scientific articles and was the co-director of two PhD students. Currently he is the co-director of 3 PhD theses. From 2011 to 2016 he led the Unidad de procesos de Ultraprecisión, in IK4-Tekniker, where he coordinates strategic actions in the field of multifunctional surfaces and characterization of materials. He has participated in 10 European projects and coordinated two of them. His group applied for 4 different patents between 2011 and 2016.

Maria Luisa Fernández-Gubieda is an expert in the field of magnetic materials being the head of the group of Magnetism and Magnetic Materials in the University of Basque Country and the leader of a research project on magnetotactic bacteria working on this project a multidisciplinary team of researchers from materials science, physics, microbiology, electronic engineering and medicine. Along her career, she has studied the correlation between structure and magnetic properties on different materials such as amorphous magnetic materials, nanogranular thin films and nanoparticle systems. One of her main activities is the use of Large Scale Facilities specially Synchrotron radiation, being one of the promoters of the beamline “Core level absorption and Emission Spectroscopies” at the Spanish synchrotron ALBA. She has published more than 100 scientific papers in peer-reviewed journals (h-index = 21) and has supervised 5 PhD

Thesis.

Jon Gutiérrez received the diploma and the doctor degree, both in physics, from the Universidad del País Vasco UPV/EHU in 1985 and 1992, respectively. He is one of the seed members of the Group of Magnetism and Magnetic Materials founded and led by Prof. J.M. Barandiarán at this university. His areas of interest cover from the study of the structure and the fundamental magnetic properties of magnetic materials to the analysis and development of possible technical applications to be implemented in sensor-like devices. One of the main focus of his research is the use of magnetoelastic amorphous ribbons for sensing purposes, and any other related device or phenomenon, like nowadays magnetoelectric laminates or functionalized magnetoelastic labels for biosensing. Dr. J. Gutiérrez has published about 130 scientific papers in peer-reviewed journals and has supervised 5 PhD Thesis. He is deeply involved with the Technical Committee of the European Magnetic Sensors & Actuators (EMSA) and Materials and Applications for Sensors and Transducers (IC-MAST) Conferences.

Maria Isabel Arriortua's (PhD 1981, UPV/EHU) interest in materials chemistry dates back to her work in the University of Lovaine-la-Neuve, where she did part of her PhD thesis. Upon returning to the University of the Basque Country, she set up the Crystallography group at this university and her work has resulted in more than 350 scientific articles (h-index: 44) and she has supervised 17 PhD Thesis. Since 1992 she has been Full Professor of Crystallography and Mineralogy at UPV/EHU and director of the UPV/EHU Advanced Research Facilities (SGIker) since its creation. She has been awarded with the Euskadi research award in Science and Technology in 2010 and coordinated the Materials Science and Technology area for the National Evaluation and Foresight Agency (ANEP) of the Spanish Government from 2010 to 2014. Nowadays she is member of the expert committee for the design of Basic Strategic Lines of Science, Technology and Innovation for the Basque Government and academic of Jakiunde, Basque Academy of Sciences, Arts and Letters since 2012. She is PI of projects related with mass and/or energy generation and storage materials, focussed on the relationship between crystal structure and properties.

Ana Catarina Lopes is graduated in Physics and Chemistry in 2006 and Master in Physics in 2009. In September 2013 she obtained her Physics PhD degree at the University of Minho (Portugal). Part of her thesis work was in collaboration with the University of Valencia, Spain and University of Münster, Germany, and dealt about electroactive polymeric composites with porous structured materials. She also performed one year Post-doc at the University of Minho, where she worked in the project of ionic electroactive polymers for high performance actuators applications. In 2016 she was awarded with a Marie Skłodowska-Curie Individual Fellowship under the project BIDMAG: “Biological detection with functionalized Magnetic Sensor” (in BCMaterials, Spain), which main objective is to develop smart hybrid surfaces of polymer functionalised for a specific bacteria binding, onto magnetic substrates (MER), able to present magnetic response to a given biological agent. She is author and co-author of 31 articles in indexed journals, receiving more than 1400 citations (h-index = 16).